# Conceptual “Progress” in Large Scale Dynamo Theory

Eric Blackman (Univ. of Rochester)

- Different styles and goals of dynamo research / analogies to accretion disk research
- Ask not: “Is mean field theory correct” BUT “Is it the correct mean field theory?”
- Classification of dynamos
- Magnetic helicity NOT kinetic helicity is the “unifying” helicity
- Seemingly different LSDs and their saturation can be unified by tracking magnetic helicity
- Textbook shortcomings vs. principles of nonlinear saturation
- Importance of time evolution, helicity fluxes, and shear
- Importance of subtle restrictions and differences between simulations
- Symbiosis between interior and coronal dynamos in astrophysics
- are key LSD properties sensitive to mechanism of reconnection?
- New “transient” dynamos for explosive astrophysics

# 1. Small Scale Dynamos

- flow driven
- no pseudo-scalar involved; EMF irrelevant
- field amplified at and below forcing scale; little amplification at $k < k_f$

# 2. Large Scale Dynamos (LSD)

- EMF essential; tracking properly defined magnetic helicity evolution potentially relevant for understanding saturation in ALL cases
- field sustained on time or spatial scales larger than turbulent forcing scales
- **Globally Reflection Asymmetric** sign of $< \overline{\mathcal{E}} \cdot \overline{B} >$ fixed by initial conditions
  - Saturation determined by coupling large scale B growth to small scale mag. helicity evolution
    - Flow Driven Helical Dynamo (FDHD): Inside Rotators
      - artificially forced or natural
      - sheared or unsheared
    - Magnetically Driven Helical Dynamo (MDHD)= Dynamical relaxation in Lab Plasmas and Coronae
- **Not GRA**: sign of $\overline{\mathcal{E}} \cdot \overline{B}$ can be finite in subaverage; helicity flux can be of fixed sign
    - stochastic large scale dynamos (e.g. Vishniac & Brandenburg 97)
    - turb+ shear w/out imposed helical forcing or pseudoscalar (Lesur & Ogilvie 08; Yousef et al 08)?
    - quasi-locally averaged finite pseudo scalars e.g. $\overline{\epsilon} \propto (\overline{\mathbf{W}} \cdot \nabla)\overline{B}^2$
    - absence of helical forcing but shear Brandenburg Sandin 04: Helicity fluxes sustain LSD

# 2A. Globally Helical LSDs

- Flow Driven (FDHD): flow energy initially exceeds mag. energy
  - FDHD: global pseudoscalar or psedovector flux of mag. helicity
  - FDHD amplifies and pumps oppositely signed magnetic helicities to large and small scales **or** drives spatial flows of mag. helicity
  - nonhelical mean field can still dominate magn energt and
  - SSD often concurrent
- Magnetically Driven (MDHD): magnetic energy exceeds kinetic energy
  - MDHD: injection of magnetic helicity
  - MDHD induces relaxation of injected sign of mag. helicity to large scales and drives velocity flows.
  - interesting ambiguity with stratified MRI and tachocline

# Laboratory Plasma Dynamos: MDHD

- injected magnetic helicity drives system away from relaxed state; MDHD fights to bring it back
- relaxed state has magnetic helicity on largest scale subject to boundary conditions
- MDHD sustains large scale field against decay
- MDHD "amplifies" large scale magnetic helicity
- analogue to astrophysical coronae: MDHD also important
- in astrophysics

# Dynamo Evolution Equations: Unifying LSDs (e.g. B07)

$$\partial_t(\mathbf{A}\cdot\mathbf{B}) = -2\eta(\mathbf{J}\cdot\mathbf{B}) - \nabla\cdot(\Phi\mathbf{B} + \mathbf{E}\times\mathbf{A})$$

$$\partial_t\overline{\mathbf{a}\cdot\mathbf{b}} = -2\overline{\boldsymbol{\mathcal{E}}}\cdot\overline{\mathbf{B}} - 2\eta\overline{\mathbf{j}\cdot\mathbf{b}} - \nabla\cdot(\overline{\phi\mathbf{b}} + \overline{\mathbf{e}\times\mathbf{a}})$$

needed to understand saturation

$$\partial_t(\overline{\mathbf{A}}\cdot\overline{\mathbf{B}}) = 2\overline{\boldsymbol{\mathcal{E}}}\cdot\overline{\mathbf{B}} - 2\eta\overline{\mathbf{J}}\cdot\overline{\mathbf{B}} - \nabla\cdot(\overline{\Phi}\,\overline{\mathbf{B}} + \overline{\mathbf{E}}\times\overline{\mathbf{A}})$$

$$\partial_t\overline{\mathbf{B}} = \nabla\times(\overline{\mathbf{V}}\times\overline{\mathbf{B}}) + \nabla\times\overline{\boldsymbol{\mathcal{E}}} + \nu_M\nabla^2\overline{\mathbf{B}}$$

choose one: bottom required when shear is important

$$\partial_t\overline{\boldsymbol{\mathcal{E}}} = \overline{\partial_t\mathbf{v}\times\mathbf{b}} + \overline{\mathbf{v}\times\partial_t\mathbf{b}}$$

$$\partial_t\mathbf{b} = \ldots$$

$$\partial_t\mathbf{v} = \ldots$$

$$\partial_t\overline{\mathbf{V}} = \ldots$$

facilitates "minimal tau" closure for dynamical theory e.g.BF02...Br-Sub05

$$\mathbf{E} = -\mathbf{V}\times\mathbf{B} + \eta\mathbf{J},$$

$$\overline{\mathbf{E}} = -\overline{\boldsymbol{\mathcal{E}}} - \overline{\mathbf{V}}\times\overline{\mathbf{B}} + \eta\overline{\mathbf{J}}$$

$$\mathbf{e} = \boldsymbol{\mathcal{E}} - \mathbf{v}\times\mathbf{b} - \mathbf{v}\times\mathbf{B} - \overline{\mathbf{V}}\times\mathbf{b} + \eta\mathbf{j}$$

# Case 1: MDHD: Tokamak Dynamo (figs from Ji &Prager 01)

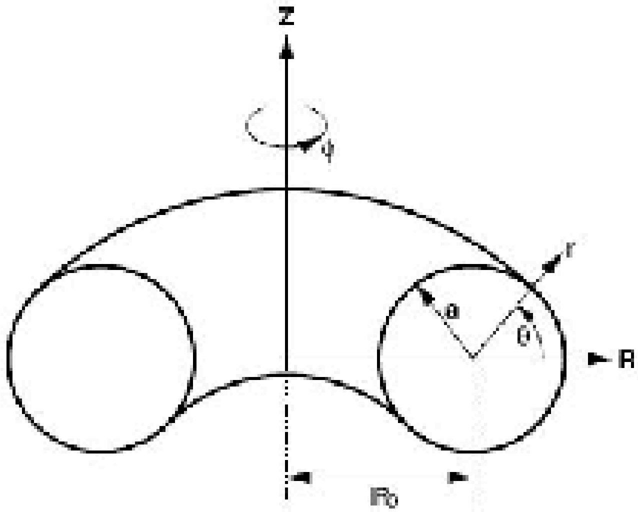


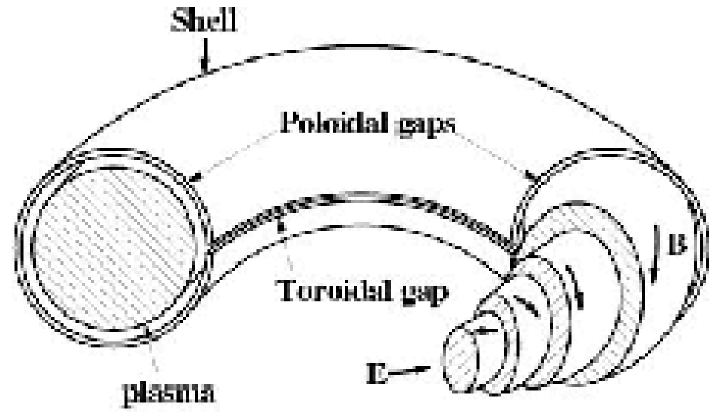


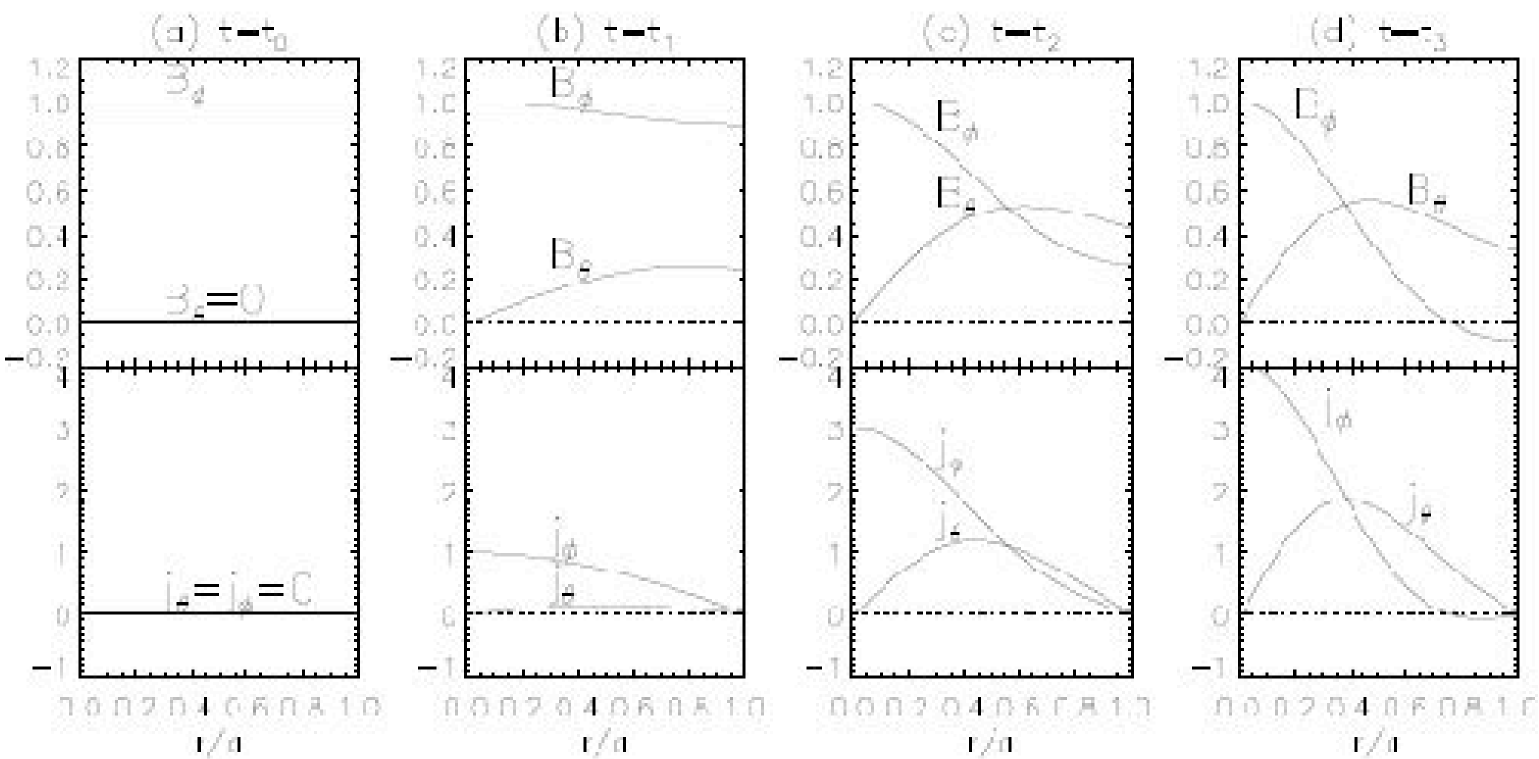

# MDHD: Tokamak Dyn (cont.)

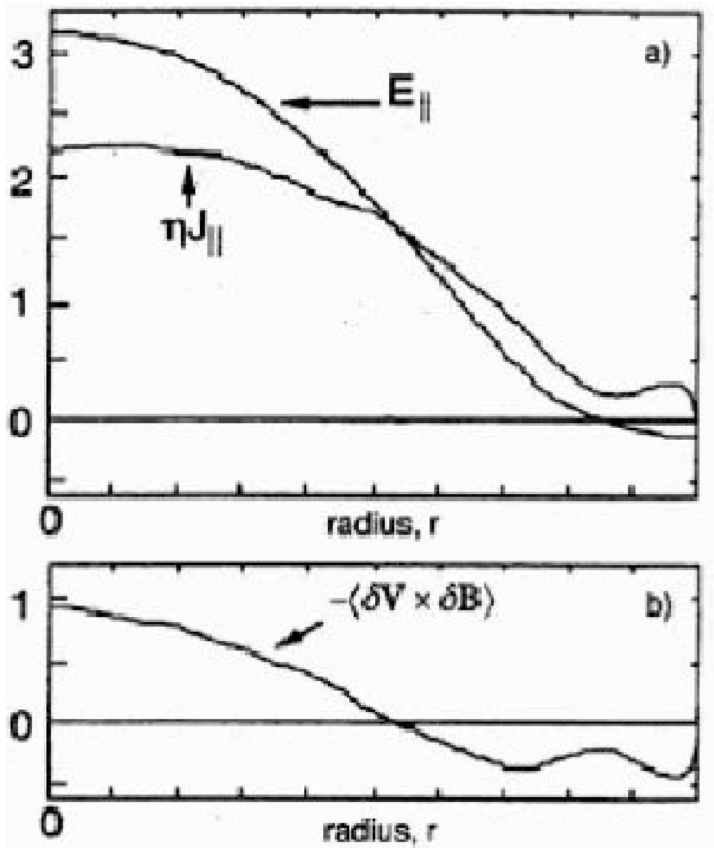


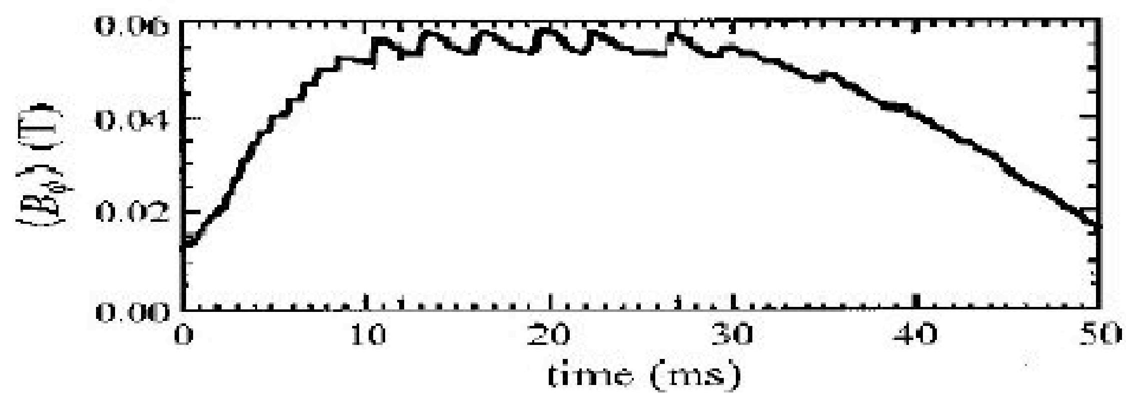

# Case 1 Tokamak Dynamo (continued)

Mean field is strong, fluctuations weak.

$$\partial_t(\overline{\mathbf{a}\cdot\mathbf{b}}) = 0 = -2\overline{\boldsymbol{\mathcal{E}}}\cdot\overline{\mathbf{B}} - \nabla\cdot(\overline{\phi\mathbf{b}} + \overline{\mathbf{e}\times\mathbf{a}}) \tag{7}$$

$$\overline{\boldsymbol{\mathcal{E}}}\cdot\overline{\mathbf{B}} = \nabla\cdot\overline{\mathbf{h}} = \eta\overline{\mathbf{J}}\cdot\overline{\mathbf{B}} - \overline{\mathbf{E}}\cdot\overline{\mathbf{B}} \tag{8}$$

$$\overline{\mathbf{E}}\cdot\overline{\mathbf{B}} = -\nabla\cdot(\overline{\Phi}\overline{\mathbf{B}} + \overline{\mathbf{E}}\times\overline{\mathbf{A}}) \tag{9}$$

Helicity Injection: e.g.

$$\int\nabla\cdot(\overline{\Phi\mathbf{B}})dV = \int\overline{\Phi\mathbf{B}}\cdot d\mathbf{S} = (\overline{\Phi}_2 - \overline{\Phi}_1)\Psi_t = V_s\Psi_t$$

$V_s$ is voltage drop, $\Psi_t$ is toroidal flux.

Integrating over the full volume:

$$\int\overline{\boldsymbol{\mathcal{E}}}_{||}\cdot\overline{\mathbf{J}}dV = \int\Lambda\overline{\boldsymbol{\mathcal{E}}}\cdot\overline{\mathbf{B}}dV = \int\Lambda\overline{\mathbf{h}}\cdot d\mathbf{S} - \int(\overline{\mathbf{h}}\cdot\nabla\Lambda)dV \simeq \int\eta\overline{\mathbf{J}}_{||}^2 dV. \tag{10}$$

When surface term vanishes, outward flux of small scale helicity ($\overline{\mathbf{h}} > 0$) is, on average, in the direction of decreasing $\Lambda \equiv \frac{\overline{\mathbf{J}}\cdot\overline{\mathbf{B}}}{\overline{B}^2}(> 0)$. Helicity flux acts to "homogenize" helicity gradient.

also Strauss 85; Bhattacharjee Hameri 86; Bellan 00; Otolani & Schnack 93

# MDHD (dynamical magnetic relaxation)

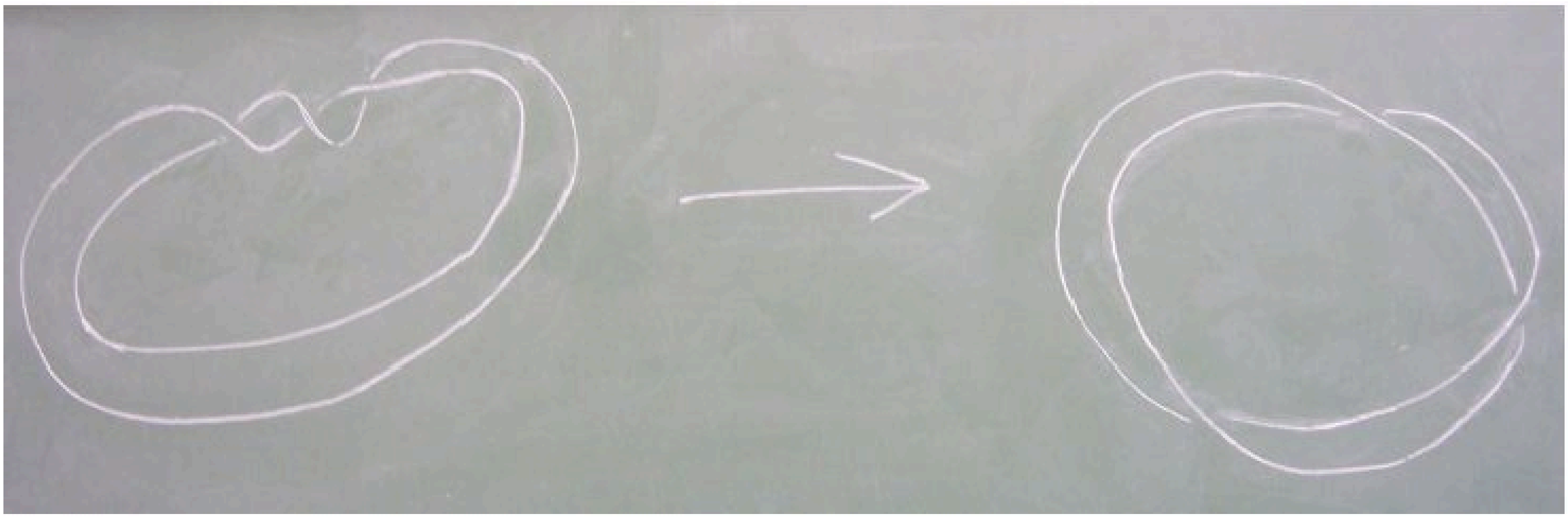

# MDHD: Spheromak and Jet Formation (cont)

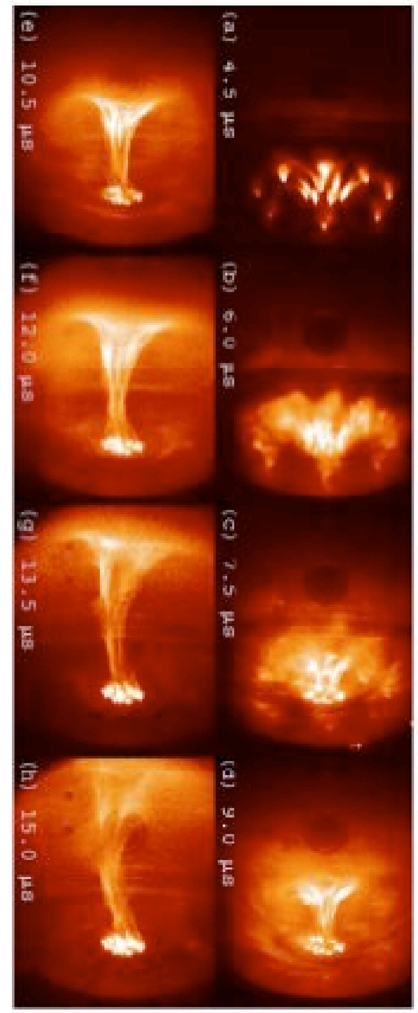


**Figure 3.** Images of plasma evolution (shot 1210; peak $\alpha_{gun} \approx 66\,\mathrm{m}^{-1}$) in which a plasma column forms and persists for many Alfvén transit times, illustrating the magnetic topology required for an astrophysical jet.

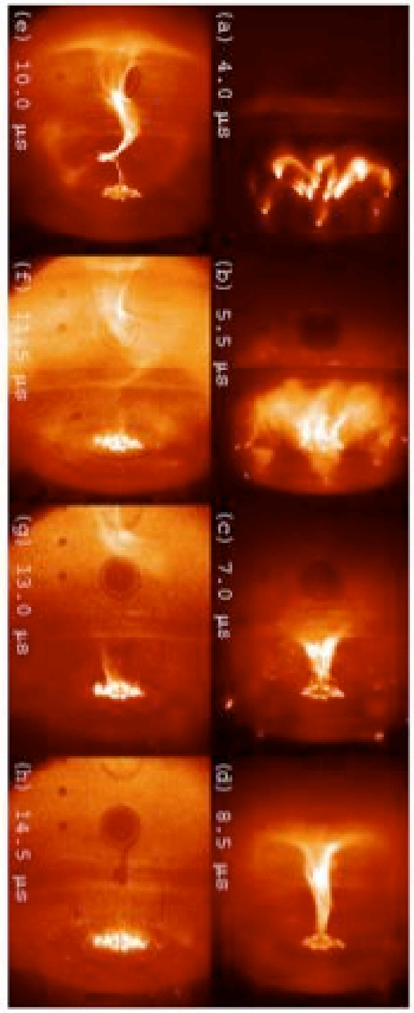


**Figure 4.** Images of plasma evolution (shot 1233; peak $\alpha_{gun} \approx 71\,\mathrm{m}^{-1}$) in which a helical instability, probably a current-driven kink, develops on the ideal MHD time-scale, illustrating one possible source of jet internal structure.

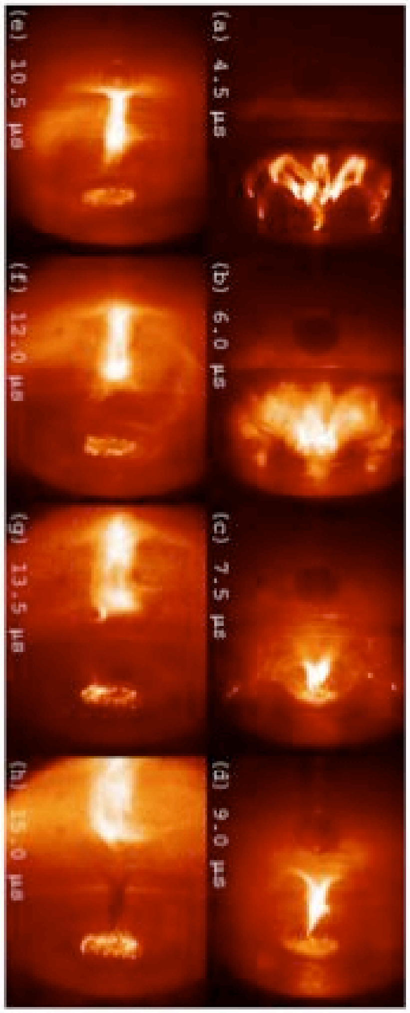


**Figure 6.** Images of plasma evolution (shot 1181; peak $\alpha_{gun} \approx 129\,\mathrm{m}^{-1}$) in which the plasma detaches from the electrodes, illustrating the possibility of field-line opening in disc coronae.

# MDHD: Spheromak and Jet Formation

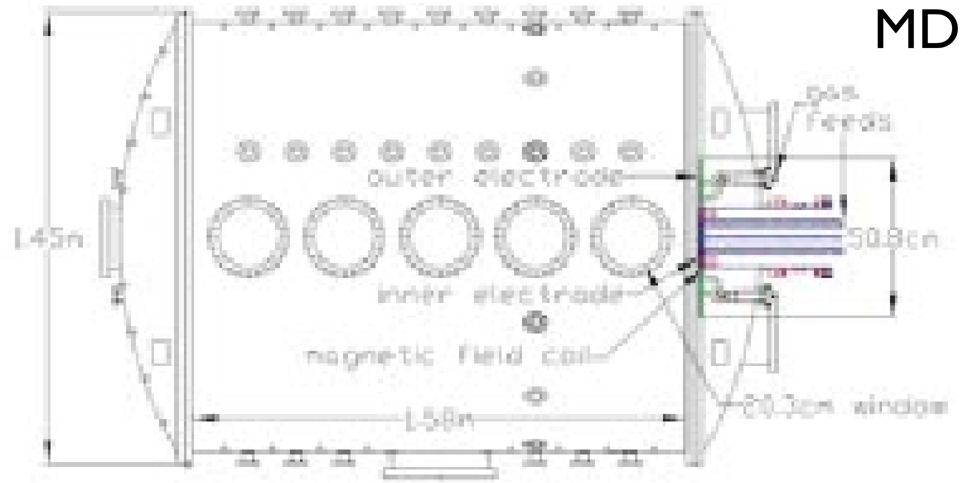


**Figure 1.** Side-view schematic of vacuum chamber and planar coaxial gun setup.

Hsu and Bellan 02

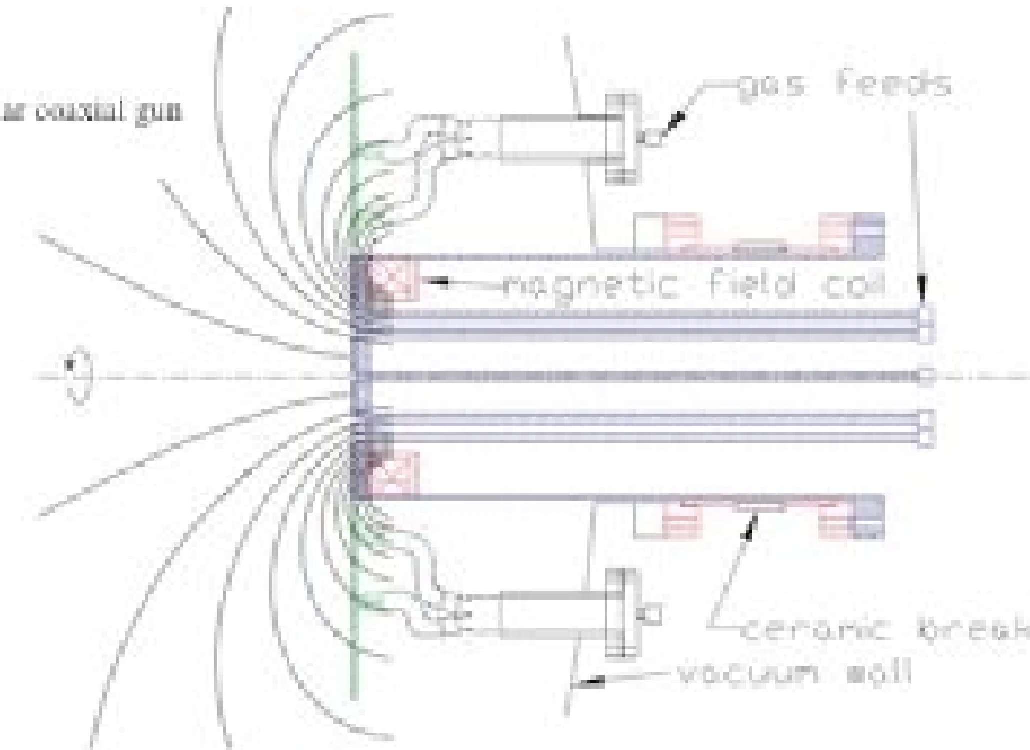


**Figure 2.** Side-view schematic of planar coaxial gun, including gas feeds, external magnetic field coil, poloidal flux $\psi$ contours and symmetry axis.

# Case 2: FDHD: $\alpha^2$ Dynamo in Periodic Box

LSD and SSD concurrent

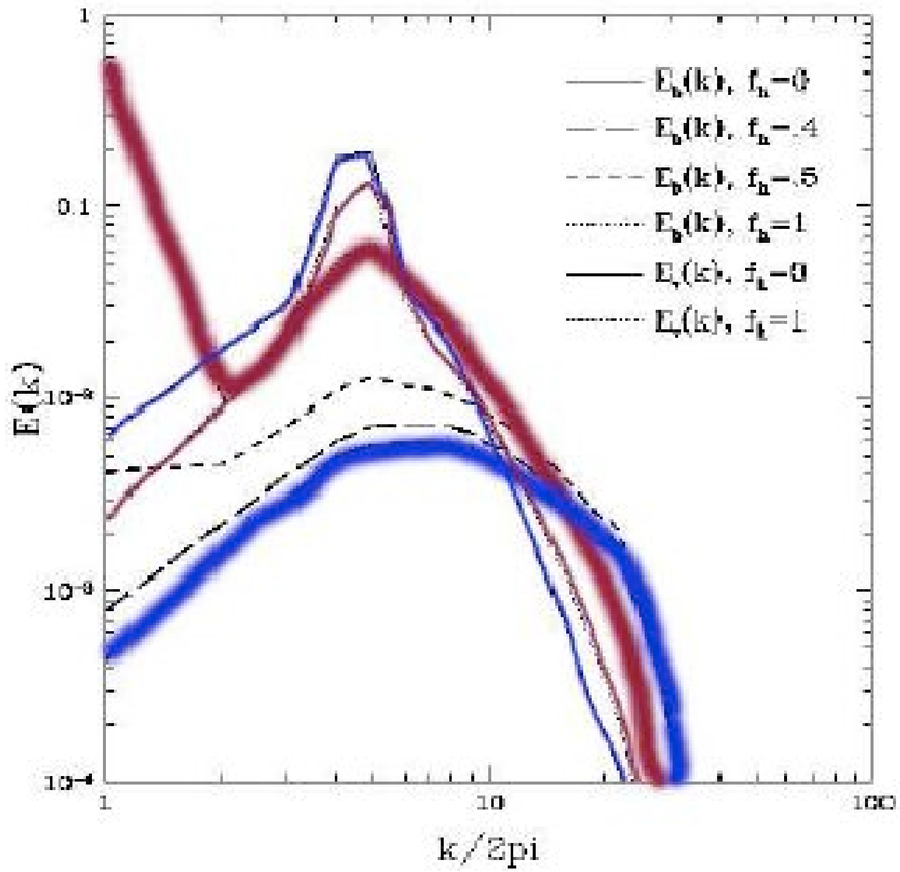


(simulation from Maron & Blackman 03; see also Brandenburg 01)

- NOTE: "**Bihelical Equilibrium**" for $f_h = 1$

# $\alpha^2$ Dynamo in Periodic Box (cont)

**Differential Equations to be solved:**

$$\partial_t\langle\overline{\mathbf{A}}\cdot\overline{\mathbf{B}}\rangle = 2\langle\overline{\boldsymbol{\mathcal{E}}}\cdot\overline{\mathbf{B}}\rangle - 2\eta\langle\overline{\mathbf{J}}\cdot\overline{\mathbf{B}}\rangle + \cancel{\nabla\cdot\langle\rangle_1}$$

$$\partial_t\langle\mathbf{a}\cdot\mathbf{b}\rangle = -2\langle\overline{\boldsymbol{\mathcal{E}}}\cdot\overline{\mathbf{B}}\rangle - 2\eta\langle\mathbf{j}\cdot\mathbf{b}\rangle + \cancel{\nabla\cdot\langle\rangle_2}$$

$$\partial_t\overline{\boldsymbol{\mathcal{E}}} = \partial_t\overline{\mathbf{v}\times\mathbf{b}} = \overline{\mathbf{v}\times\partial_t\mathbf{b}} + \overline{\partial_t\mathbf{v}\times\mathbf{b}}$$

$$= -\tfrac{1}{3}(\overline{\mathbf{v}\cdot\nabla\times\mathbf{v}} - \overline{\mathbf{b}\cdot\nabla\times\mathbf{b}})\overline{\mathbf{B}} - \tfrac{1}{3}\overline{\mathbf{v}^2}f(\overline{\mathbf{B}})\nabla\times\overline{\mathbf{B}} - \overline{\mathbf{v}\times\mathbf{b}}/\tau$$

$$\partial_t\mathbf{b} = -\nabla\times\mathbf{e} = \nabla\times(\mathbf{v}\times\overline{\mathbf{B}}) + \nabla\times(\mathbf{v}\times\mathbf{b}) - \nabla\times\overline{\mathbf{v}\times\mathbf{b}} + \eta\nabla^2\mathbf{b} + g(\overline{\mathbf{V}})$$

$$\partial_t\mathbf{v} = \mathbf{f} - \mathbf{v}\cdot\nabla\mathbf{v} + \overline{\mathbf{v}\cdot\nabla\mathbf{v}} - \nabla p + \mathbf{j}\times\overline{\mathbf{B}} + \overline{\mathbf{J}}\times\mathbf{b} + \mathbf{j}\times\mathbf{b} - \overline{\mathbf{j}\times\mathbf{b}} + \nu\nabla^2\mathbf{v} + f(\overline{\mathbf{V}})$$

- <u>minimal $\tau$</u> closure for triple corr. in $\partial_t\overline{\boldsymbol{\mathcal{E}}}$ (used in BF02 (dynamo),BF03 (scalar diffusion)) (note also: Vainshstein Kitchatinov 83;Kleeorin + al. 96,Raedler + al.03)
  $\tau$ is damping time, not correl. time.

- <u>No first order smoothing needed</u>

# $\alpha^2$ Dynamo in Periodic Box (cont)

$$\partial_t H_1^M = \frac{2k_1\tau}{3}\left(k_2^2 H_2^M - H_2^V\right) H_1^M - 2\beta k_1^2 H_1^M - 2\nu_M k_1^2 H_1^M$$

$$\partial_t H_2^M = -\frac{2k_1\tau}{3}\left(k_2^2 H_2^M - H_2^V\right) H_1^M + 2\beta k_1^2 H_1^M - 2\nu_M k_2^2 H_2^M$$

$$\partial_t H_2^V = 0$$

- Helical velocity driven dynamo "pumps" magnetic helicity of one sign to large scales and the other sign to small scales

# $\alpha^2$ Dynamo in Periodic Box (cont)

**Large Scale Helical Field Growth:** 2-scale (Blackman & Field 02) vs. empirical fit formula of Brandenburg (01) Curves left to right: $R_M = 100, 250, 500$: $h_1$ normalized Large scale magnetic helicity.

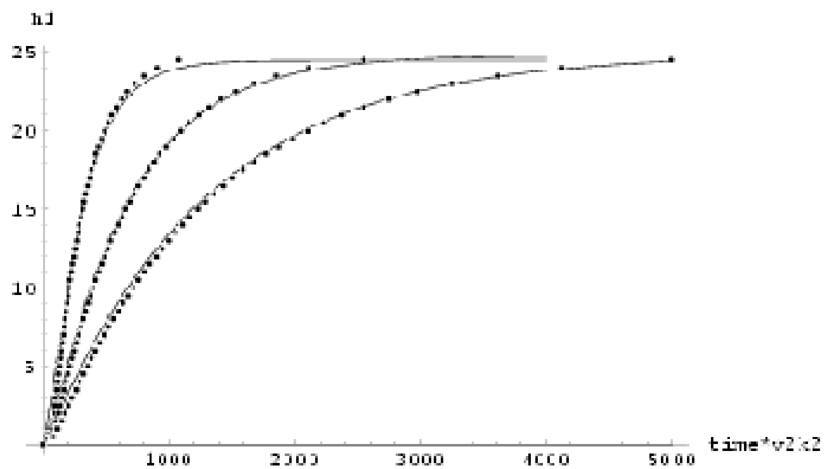


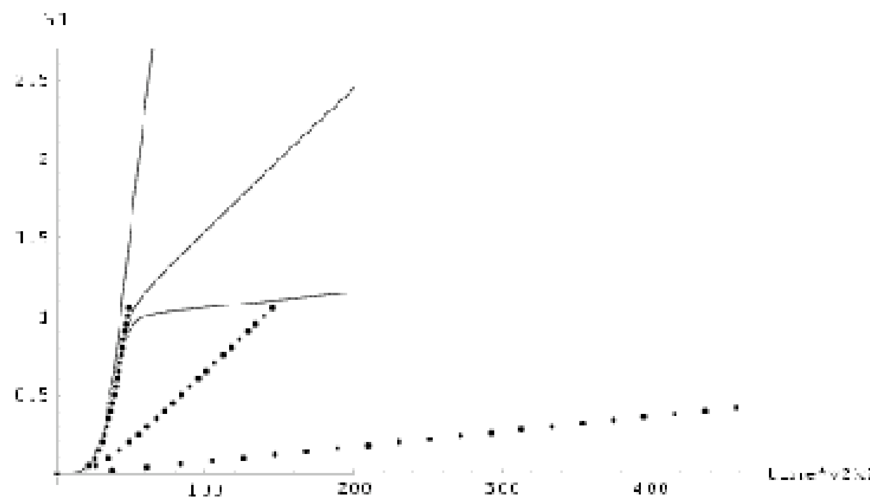


- At end of kinematic regime: $\overline{\mathbf{B}}^2 \sim f_h v_2^2 \left(\frac{k_1}{k_2}\right)$
- At end of resistive regime: $\overline{\mathbf{B}}^2 \sim f_h v_2^2 \left(\frac{k_2}{k_1}\right)$

## MULTI-SCALE THEORY (B03;B05)

$$\partial_\tau h_1 = \frac{2}{3}\left(f_h + h_2 + \left(\frac{k_3}{k_2}\right)^{\frac{4}{3}} h_3\right)\frac{k_1}{k_2}h_1 - 2\left(\frac{q(h_1)}{3} + \frac{q(h_1)}{3}\left(\frac{k_2}{k_3}\right)^{\frac{4}{3}} + \frac{1}{R_M}\right)\left(\frac{k_1}{k_2}\right)^2 h_1 \quad (11)$$

$$\begin{aligned}\partial_\tau h_2 = \frac{-2}{3}\left(\frac{k_3}{k_2}\right)^{\frac{4}{3}} f_u h_3 h_2 - \frac{2}{3}\left(f_h + h_2\right)\frac{k_1}{k_2}h_1 + \frac{2q(h_1)}{3}\left(\frac{k_1}{k_2}\right)^2 h_1 \\ -2\left(\frac{q(h_1)}{3}g_u\left(\frac{k_2}{k_3}\right)^{\frac{4}{3}} + \frac{1}{R_M}\right)h_2\end{aligned} \quad (12)$$

and

$$\begin{aligned}\partial_\tau h_3 = \frac{2}{3}\left(\frac{k_3}{k_2}\right)^{\frac{4}{3}} f_u h_3 h_2 - \frac{2}{3}\left(\frac{k_3}{k_2}\right)^{\frac{4}{3}}\left(\frac{k_1}{k_2}\right)h_3 h_1 + \frac{2q(h_1)}{3}\left(\frac{k_2}{k_3}\right)^{\frac{4}{3}}\left(\frac{k_1}{k_2}\right)^2 h_1 \\ + \frac{2q(h_1)}{3}g_u\left(\frac{k_2}{k_3}\right)^{\frac{4}{3}} h_2 - \frac{2}{R_M}\left(\frac{k_3}{k_2}\right)^2 h_3\end{aligned} \quad (13)$$

**At end of fast growth regime:**

$$h_1 \simeq 1 - (k_2/k_3)^{4/3} + (k_2/k_3)^{8/3} \quad (14)$$

$$h_2 \simeq -1 + (k_2/k_3)^{4/3} \quad (15)$$

and

$$h_3 \simeq -(k_2/k_3)^{8/3} \quad (16)$$

# 3-scale approach justifies 2 scale approach:

"Small scale" mag and current helicity initially peaks at tiny scales, but quickly inverse transfers to forcing scale before kinematic regime ends

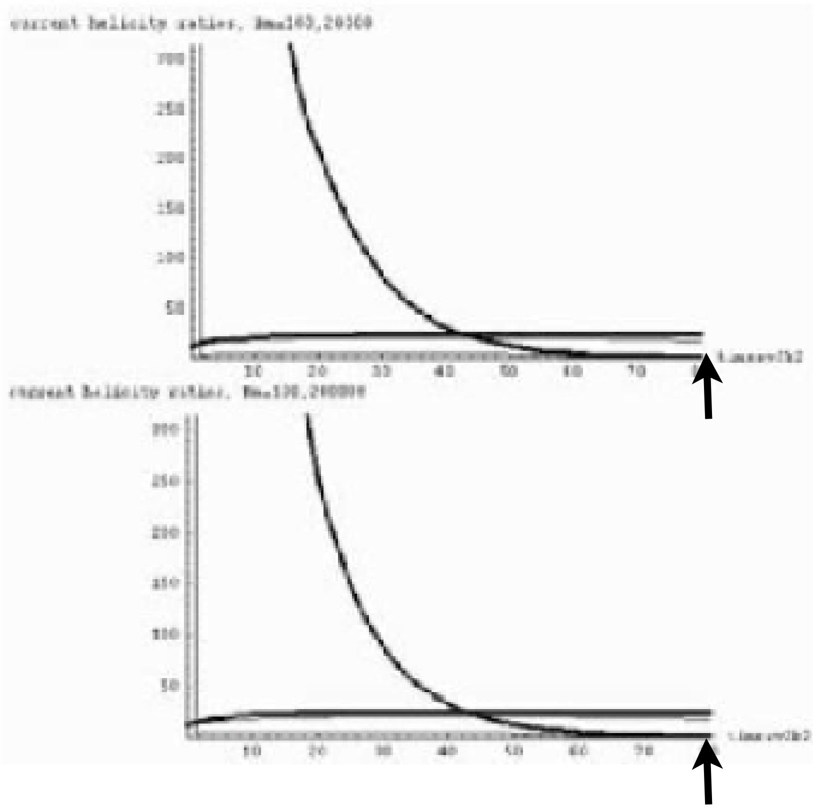

$$\frac{k_3^2 h_3}{k_2^2 h_2} = \left(\frac{k_2}{k_3}\right)^{2/3}$$

**Figure 3.** The absolute magnitude of the current helicity ratios $|k_2^2 h_2/k_1^2 h_1|$ and $|k_3^2 h_3/k_1^2 h_1|$, and helical magnetic energy ratios $|k_2 h_2/k_1 h_1|$ and $|k_3 h_3/k_1 h_1|$ assuming an initial seed of $h_2(0) = h_3(0) = -h_1(0)/2 = 0.0005$, for $k_1 = 1$, $k_2 = 5$, $k_3 = 160$. The top row shows plots for $R_M = 100$ (thin lined curves) and $R_M = 2 \times 10^4$ (thick lined curves) and the bottom row shows plots for $R_M = 100$ (thin lined curves) and $R_M = 2 \times 10^5$ (thick lined curves). In each plot, the quantities at $k_3$ dominate at early times, but then become subdominant to the values at $k_2$ at later times. The magnetic energy plot is shown for a broader time range. The location of the crossover for the large-$R_M$ cases of $2 \times 10^4$ and $2 \times 10^5$ is independent of $R_M$: the crossovers occur for the thick pairs of lines at the same time in the top and bottom rows. The crossover occurs much earlier for $R_M = 100$ because the resistive wavenumber is closer to $k_3$ and thus the resistivity is more effective at early times in draining the current helicity and magnetic energy at $k_3$ than in the larger-$R_M$ cases. For the current helicity, the crossover for $R_M = 100$ occurs so early that it is not visible on the graph. Before the end of the kinematic regime ($t \lesssim 100$), the crossovers are complete and $k_2$ emerges as the dominant small scale. Since $k_3 = 160$ here, $R_M = 100$ corresponds to $Pr_M \simeq 1$.

# Lessons from $\alpha^2$ in periodic box

- coupling small scale magnetic helicity evolution into theory correctly predicts the saturation; two scale model works well
- $$\alpha = \frac{\alpha_0 + R_M\left(\frac{\beta\overline{\mathbf{J}}\cdot\overline{\mathbf{B}}}{B_{eq}^2} - \cancel{\frac{\nabla\cdot\mathbf{F}}{2k_f B_{eq}^2}} - \frac{\partial\alpha/\partial t}{2\nu_M k_f^2}\right)}{1 + R_M\overline{B}^2/B_{eq}^2}$$
- reduces to Cattaneo & Hughes 96 Gruzinov & Diamond 94 for steady state uniform field (note also Kleeorin & Ruzmaikin 82)
- simulations and theory agree in dynamical evolution but early times warrant better resolution to isolate kinematic from resistive regime
- kinematic growth produces significant LS field before resistive regime
- this kinematic regime is not necessarily enough; would like avoidance of resistively limited regime
- alleviating SS mag helicity buildup is key to avoid catastrophic quenching. This is facilitated with shear and helicity fluxes

**BOUNDARY TERMS**

• Effect of a adding **loss** term proportional to $H_2$ on the growth of $H_1$ for three different values of loss. From top to bottom, these factors are $10, 5$ and $1(=$no loss$)$, respectively. Here $R_M = 200$ and $k_2/k_1 = 5$.

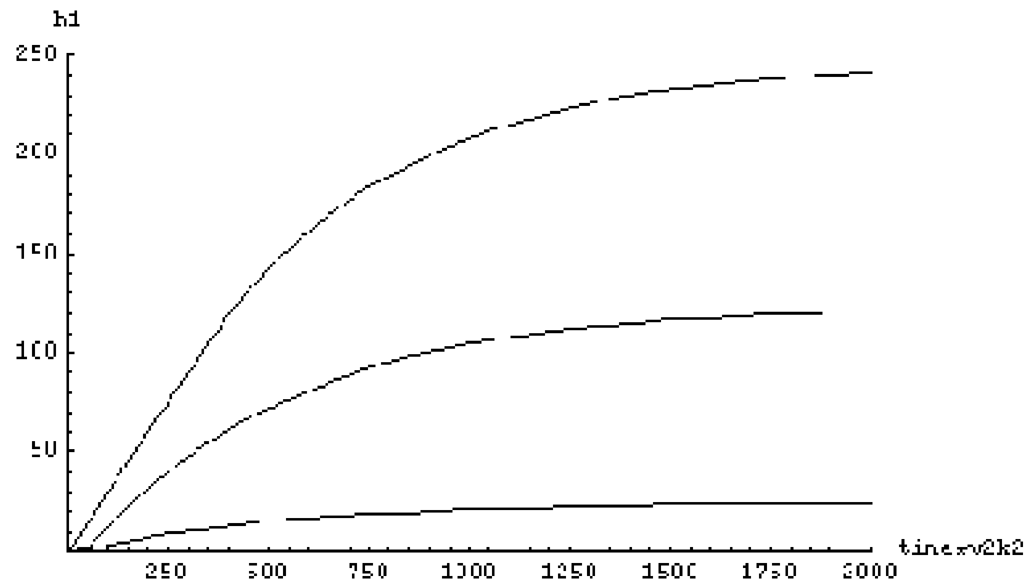


- loss of SS mag helicity helpful but both large and ss losses expected (Blackman & Field 00ab; Blackman & Brandenburg 03)
- cycle could remain fast even if saturated large scale field reduced.
- understand the relative losses in a real system self-consistently
- Brandenburg & Sandin 04: open boundaries + shear required

# Case 3: FDHD with helicity fluxes and shear

- Vishniac-Cho flux (01), recast by Subramanian & Brandenburg (04,06); flux along surfaces of cons. shear $F_{VC,i} \propto \epsilon_{ink} S_{nj} B_j B_k$
  $(S_{nj} \equiv \partial_n \overline{V}_j - \partial_j \overline{V}_n)$
- advective flux (Shukurov et al. 06) $F_{ad,i} \propto \alpha_m \overline{U}_i$
- Numerical evidence supports that SS helicity fluxes facilitate fast, robust LSD action when shear is present:
  - e.g. Brandenburg & Sadin 04 + Br-Sub 05+..: VC flux in forced turbulence with shear in solar like rotation profile with and without forcing kinetic helicity sustains LSD; shear required
  - e.g. Kapyla et al. 2008: LSD from convection + shear with surfaces of constant shear aligned toward open boundaries; Tobias et al. (08): no LSD under similar conditions BUT shear is aligned toward periodic boundaries disallowing $\boldsymbol{F}_{vc}$

# Case 3 (cont): Time dependent $\alpha-\Omega$ with helicity flux

Galactic dynamos with Shear and small scale helicity fluxes (Shukurov et al. 2006; Sur et al 2007):

$$\mathcal{E} = \alpha\overline{B} - \eta_t\overline{J}$$

$$\alpha = \alpha_K + \alpha_m$$

$$\alpha_m = \frac{1}{3}\rho^{-1}\overline{\tau j \cdot b}$$

$$\frac{\partial\overline{B}_r}{\partial t} = -\frac{\partial}{\partial z}\left(\overline{U}_z\overline{B}_r + \mathcal{E}_\phi\right) + \eta\frac{\partial^2\overline{B}_r}{\partial z^2},$$

$$\frac{\partial\overline{B}_\phi}{\partial t} = -\frac{\partial}{\partial z}\left(\overline{U}_z\overline{B}_\phi - \mathcal{E}_r\right) + \eta\frac{\partial^2\overline{B}_\phi}{\partial z^2} + q\Omega_0\overline{B}_r.$$

$$\frac{\partial\alpha_m}{\partial t} = -2\eta_t k_0^2\left(\frac{\mathcal{E}\cdot B}{B_{eq}^2} + \frac{\alpha_m}{R_m}\right) - \nabla\cdot\left(\alpha_m\overline{U}\right)$$

$$\overline{B}_r = \overline{B}_\phi = 0 \quad \text{at } z = \pm h.$$

$$C_U = \frac{U_0}{\eta_t k_1},\quad C_\Omega = \frac{\Omega_0}{\eta_t k_1^2},\quad C_\alpha = \frac{\alpha_0}{\eta_t k_1}$$

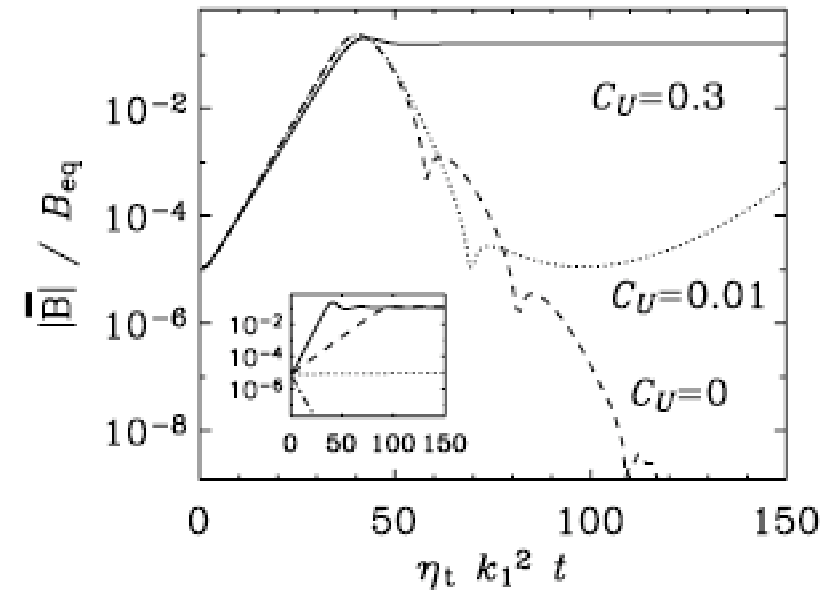


**Fig. 1.** Evolution of the field strength at $z = 0$ obtained by solving Eqs. (4)–(7) with vertical advection (solid line, $C_U = 0.3$) and without it (dashed line, $C_U = 0$), for $C_\Omega = -2$, $C_\alpha = 1$ and $R_m = 10^5$. The dynamo is neutrally stable at $C_\alpha = 0.26$ for $C_U = 0.3$ and $C_\Omega = 2$. The dotted curve, obtained for $C_U \ll 1$, shows that even weak advection can affect the long-term evolution of magnetic field. For $C_U = 0$, nonlinear effects make the $\alpha$ profile flatter at small $|z|$; this causes an oscillatory decay of the field. The inset shows similar results for $C_U$ = 0.1 (solid), 1.5 (dashed), 2 (dotted) and 3 (dash-dotted).

## HELICAL DYNAMO: REVISING THE "TEXTBOOK" PICTURE

(Blackman & Brandenburg 03)

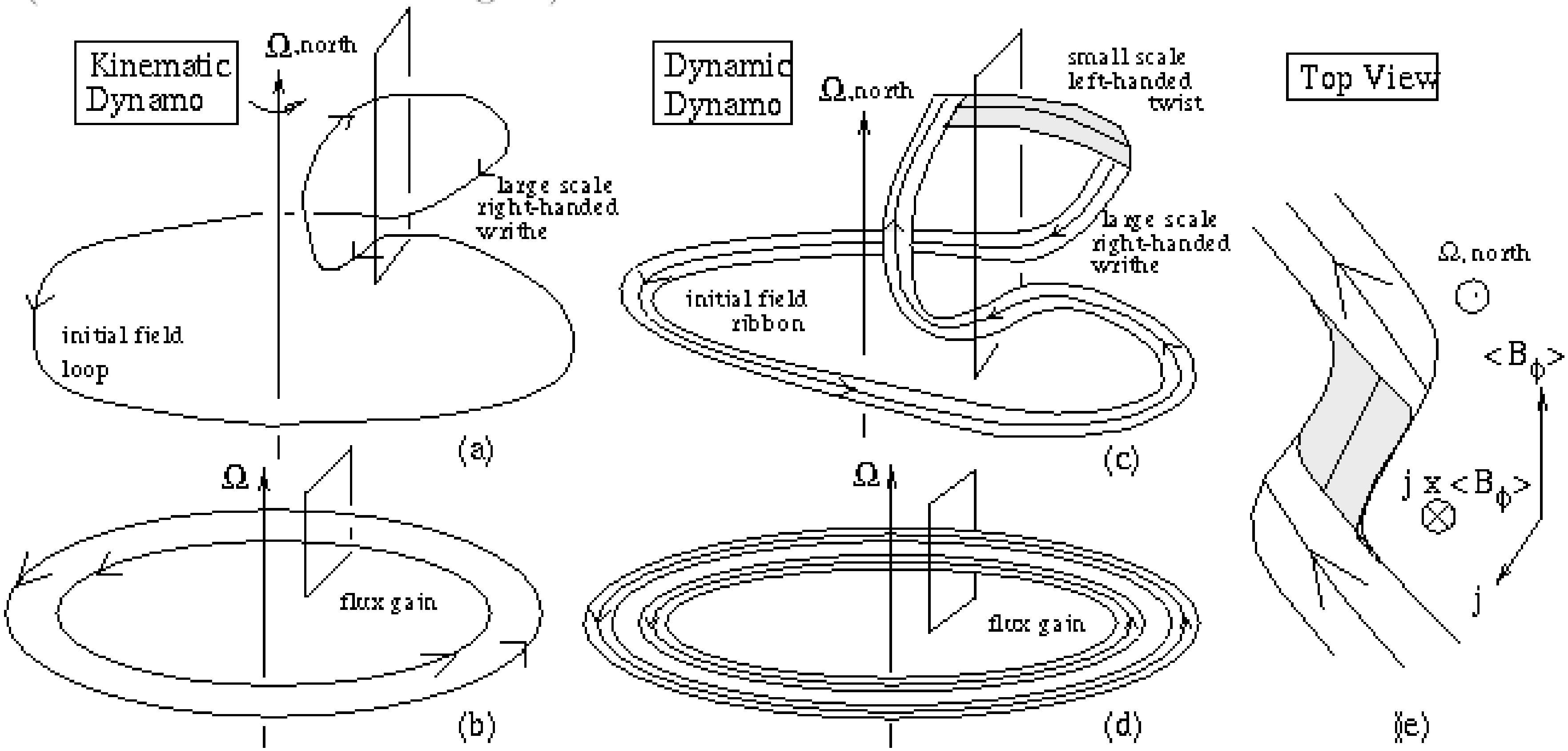

TRACE Image of a Sigmoid (Gibson et al. 2003) (195 Å)

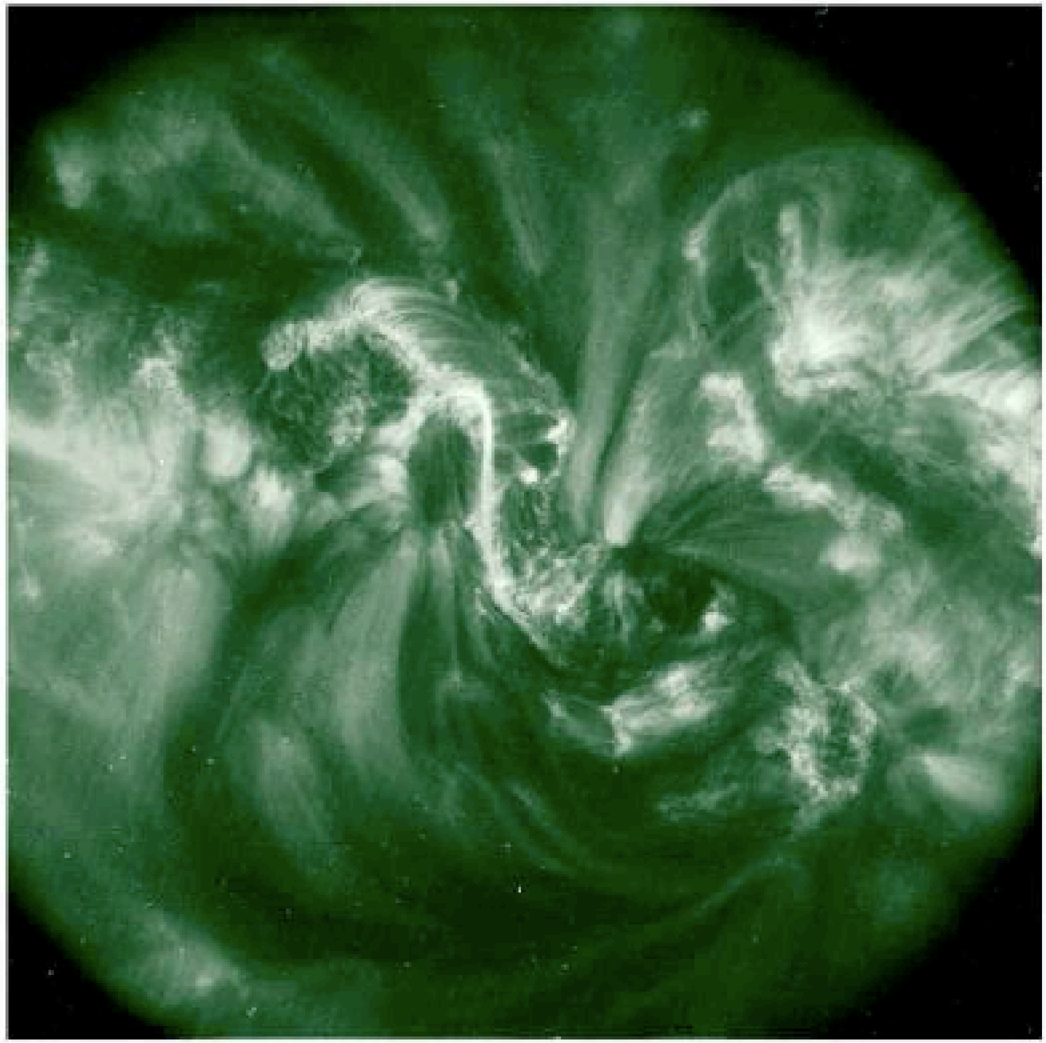

## MAGNETIC HELICITY INJECTION INTO A CORONA

- Relative helicity injection

$$\frac{dH_c}{dt} = -2\int_c \mathbf{E}\cdot\mathbf{B}dV_c + 2\int_c (\mathbf{E}\times\mathbf{A}_p)\cdot d\mathbf{S} \tag{1}$$

$$= -\frac{1}{2\pi}\int\int_{\mathbf{B}_n\cdot\mathbf{B}'_n>0}\frac{d\theta}{dt}B_nB'_ndSdS' + \frac{1}{2\pi}\int\int_{\mathbf{B}_n\cdot\mathbf{B}'_n<0}\frac{d\theta}{dt}|B_nB'_n|dSdS' \tag{2}$$

$$= \frac{dH_r}{dt}(\mathbf{twist}) \qquad + \qquad \frac{dH_r}{dt}(\mathbf{writhe}) \tag{3}$$

(e.g. Berger & Ruzmaikin 2000; Demoulin et al. 2002, 2003)

**Solar Corona Observational Issues**

• polarity from Zeeman; $\mathbf{B}_t$ is tricky
• $C = \langle \mathbf{J} \cdot \mathbf{B} \rangle$ gives handedness; $C$ vs. $H_r$ and issue wrt $\lambda$
• Chae (01,04); Local Correlation Tracking (LCT) technique for measuring helicity injection (see also Shuck 2005; Lim et al. 2007, compare LCT and LFFF)

• Observed twist and writhe have **opposite** signs. Invariant w/solar cycle (Rust & Kumar 1996, Pevtsov et al. 2001)
• **Writhe trends**: **N** (+ =r.h.) in north; **S** (− =l.h.) in south
• **Twist trends**: l.h. in north; r.h. in south
• Twist on smaller scale than writhe
$\rightarrow$ *What sign of helicity is injected in a given hemisphere?* BOTH

• Further subtlety: $H\alpha$ filaments exhibit "dextral" (r.h.) twist in North and "sinistral" (l.h.) in south (Martin & McAllister 1994+)
**But** r.h. $H\alpha$ filaments are supported by l.h. fields (Rust 1999)

# Case 4: MDHD $\alpha^2$ dynamo (dynamical magnetic relaxation)

(Blackman & Field 03, Blackman 05)

**Equations for Driven Two-Scale Helical Dynamo**

$$\partial_t H_1^M = \frac{2k_1\tau}{3}\left(k_2^2 H_2^M - H_2^V\right) H_1^M - 2\beta k_1^2 H_1^M - 2\nu_M k_1^2 H_1^M$$

$$\partial_t H_2^M = -\frac{2k_1\tau}{3}\left(k_2^2 H_2^M - H_2^V\right) H_1^M + 2\beta k_1^2 H_1^M - 2\nu_M k_2^2 H_2^M$$

$$\partial_t H_2^V = 0$$

**Equations for Driven Unihelical Magnetic Relaxation**

$$\partial_t H_1^M = \frac{2k_1\tau}{3}\left(k_2^2 H_2^M - H_2^V\right) H_1^M - 2\beta k_1^2 H_1^M - 2\nu_M k_1^2 H_1^M$$

$$\partial_t H_2^M = 0$$

$$\partial_t H_2^V \simeq \frac{2k_1\tau}{3} k_2^2\left(k_2^2 H_2^M - H_2^V\right) H_1^M - 2\beta k_2^2 k_1^2 H_1^M - 2\nu k_2^2 H_2^V$$

- Unihelical relaxation drives injected magnetic helicity to large scales

# Driven Unihelical Relaxation (Blackman Field 03,Blackman 05)

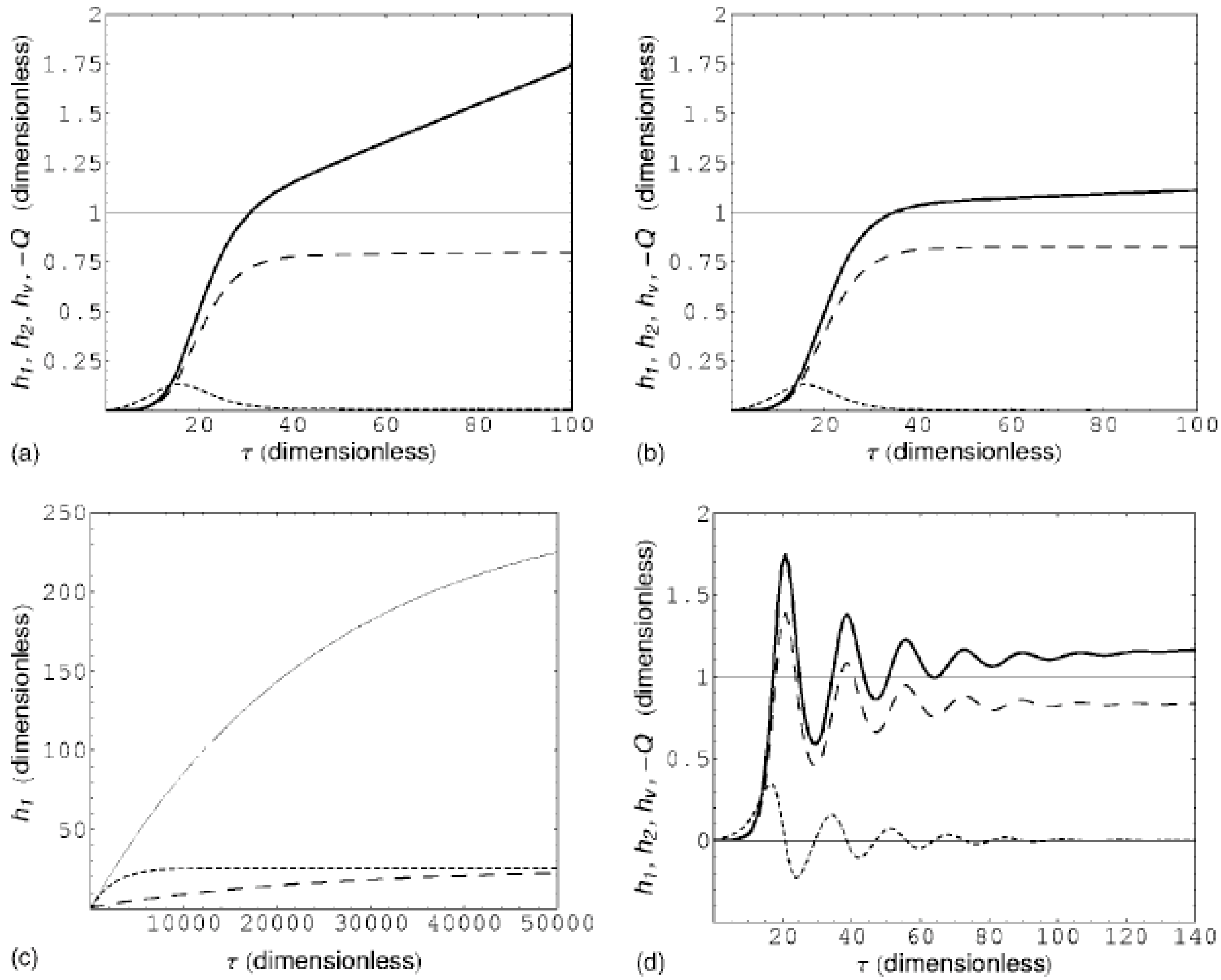


FIG. 2. (a) Same as Fig. 1(a), but case C2: fixed $h_2=1$. (b) Same as Fig. 1(b), but case C2: fixed $h_2=1$. (c) $h_1$ in case C2 for late times: solid curve is for $R_M=2000$, $R_V=200$; short dashed curve is for $R_M=R_V=200$; long dashed curve is for $R_M=R_V=2000$. (d) Same as (b), but with $f=1/10$. Notice that $-Q$ now oscillates about 0. The curves in (a) and (b) are identified as follows: At late times (not shown) the oscillations damp, and the solutions are indistinguishable from the $f=1$ case.

# Free Unihelical Relxation

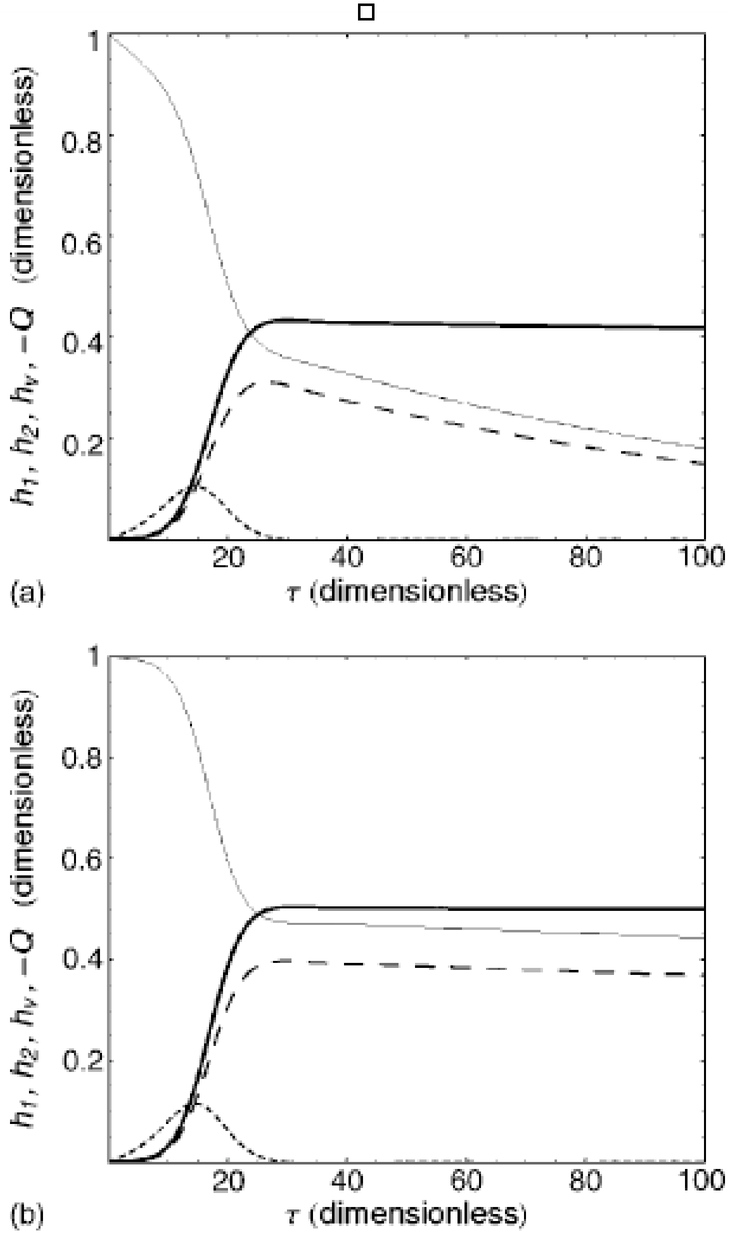


FIG. 1. Solutions for $k_1=1$, $f=1$, $k_2=5$, (a) $R_M=R_V=200$, case C1: $h_2$ free (b) $R_M=R_V=2000$, case C1: $h_2$ free. The curves in (a) and (b) are identified as follows: $h_1$ is the thick solid line, $h_2$ is the thin solid line, $h_v$ is the long dashed line, $-Q$ is the short dashed line.

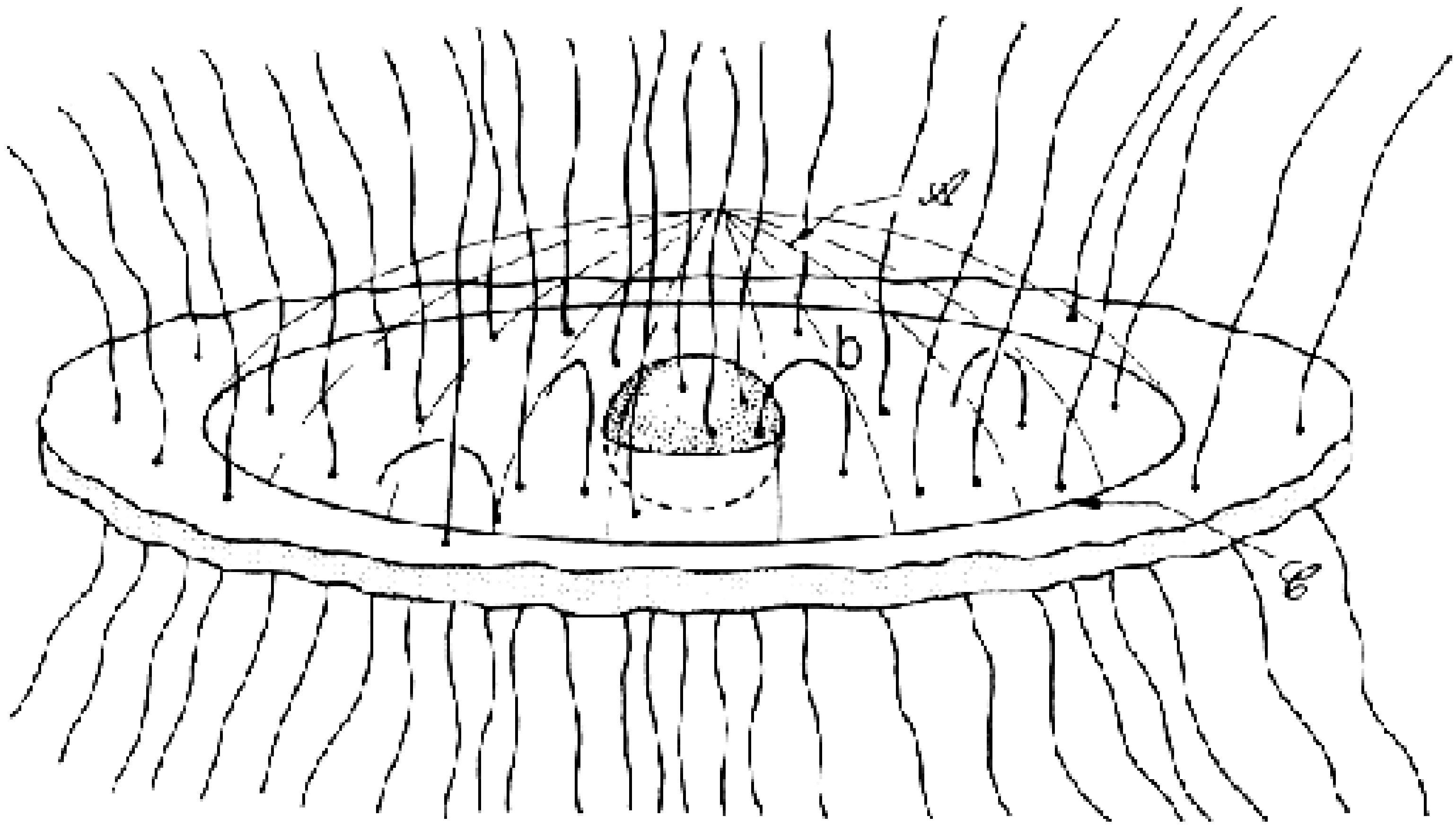


(Thorne et al. 1986)

# Jets: Interior + Exterior Dynamos

- consensus: astrophysical jets are result of magnetically mediated launch at unresolved scales less than 50 $R_{engine}$
- ironically: less consensus on relative strength of magnetic fields on observable scales > 50 $R_{launch}$
- Suggest at least jet launch is the end state of coupled helical dynamos: FDHD fields from disk escape to corona where they open up to even larger scales via MDHD; analogue to lab plasmas
- "large" scale with respect to disk is "small scale" with respect to corona
- analogue in solar corona: couple interior and exterior dynamos to get global scale fields

## Do LSD large $R_m$ dynamos depend on details of reconnection?

- Topology? : not so much
  - Mean field is degenerate with respect to SS topology
  - Mean field topology can change fast: effective $R_m$ of "mean field" in turbulent flow is large
- On getting rid of SS mag energy? very indirectly
  - turbulent cascade takes non-helical mag. energy down to resitive scales quickly preventing "lock up"; structures develop to accomodate forcing rate
  - fast robust LSD requires alleviating the buildup of SS helicity, and fluxes do this faster than local reconnection
  - helicity from interior to exterior can be dissipated by reconnection in corona

# Transient Large Scale Dynamos + Poynting Flux

(Blackman et al. 06; Nordhaus et al. 07)

(Context: Supernovae, pre-Planetary Nebulae, GRB..)

E.G. Blackman et al. / New Astronomy 11 (2006) 452–464 461

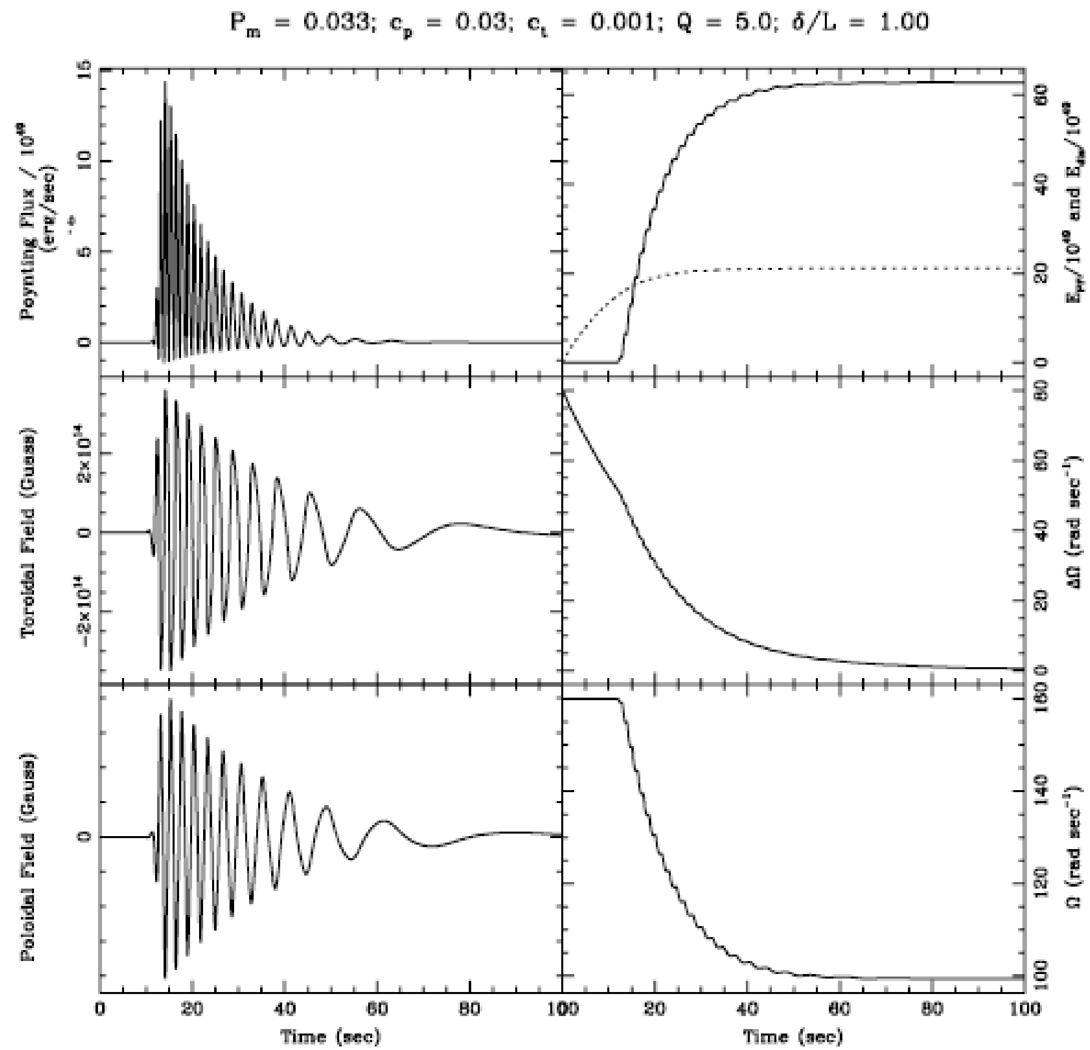


Fig. 4. Similar to Figs. 1 and 2 but with the parameters of row 17 in Table 1. This is an example of a model in which energy due to turbulent dissipation is large at early times after which magnetic energy dominates. In this case, 100% of energy in the rotational layer is available for field growth.